JCTC Journal of Chemical Theory and Computation

High-Level ab Initio Calculations To Improve Protein Backbone Dihedral Parameters

Hideaki Fujitani,* Azuma Matsuura, Sino Sakai, Hiroyuki Sato, and Yoshiaki Tanida

Fujitsu Laboratories Ltd., 10-1 Morinosato-Wakamiya, Atsugi 243-0197, Japan

Received December 8, 2008

Abstract: We present new molecular mechanical dihedral parameters for the Ramachandran angles ϕ and ψ of a protein backbone based on high-level ab initio molecular orbital calculations for hydrogen-blocked or methyl-blocked glycine and alanine dipeptides. Fully relaxed 15° (ϕ, ψ) contour maps were calculated at the MP2/6-31G(d) level of theory. Finding out the lowest energy path for ϕ (or ψ) to change from −180° to 180° in the contour map, we performed a DF-LCCSD(T0)/Aug-cc-pVTZ//DF-LMP2/Aug-cc-pVTZ level calculation to get the torsional energy profiles of ϕ (or ψ). Molecular mechanical torsion profiles with AMBER force field variants significantly differed from the ab initio profiles, so we derived new molecular mechanical dihedral parameters of a protein backbone to fit the ab initio profiles.

1. Introduction

Structural, dynamical, and equilibrium thermodynamic properties of biological macromolecules such as proteins and nucleic acids are commonly studied by molecular mechanics and molecular dynamics simulations. But their usefulness depends critically on the adequacy of the empirical force field parameters such as atomic charges, van der Waals parameters, and bond parameters. In the 1990s, Kollman's group developed a second generation of the Assisted Model Building with Energy Refinement (AMBER) force field for the simulation of proteins, nucleic acids, and organic molecules in condensed phases.[1] In addition to improvements in the parameters, they tried to explicitly describe the algorithm by which those parameters were derived, so that consistent extensions could be made to molecules other than proteins.

The peptides *N*-acetyl-*N*′-methylglycinamide and *N*-acetyl-*N*′-methylalaninamide have been widely studied. As they show conformational variations similar to proteins, they are considered model peptides for studying the character of Ramachandran angles ϕ and ψ (Figure 1). They are referred to as glycine dipeptide (GD) and alanine dipeptide (AD), respectively. Molecules such as α-(formylamino)ethanamide and (*S*)-α-(formylamino)propanamide have also been studied since they are formed from GD and AD by replacing the terminal methyl groups with hydrogen atoms. They are referred to as glycine dipeptide analogue (GDA) and alanine dipeptide analogue (ADA), respectively.

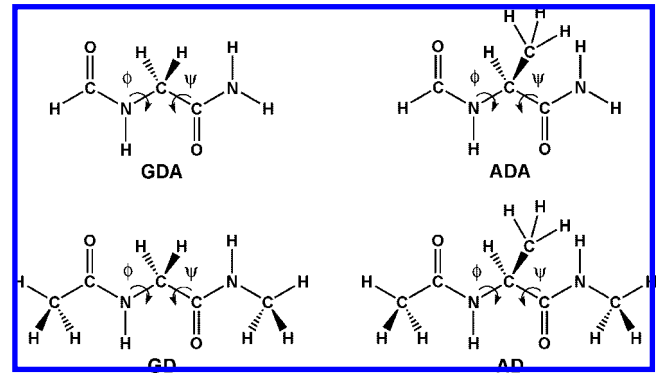

Figure 1. The structures of α-(formylamino)ethanamide (GDA), *N*-acetyl-*N*′-methylglycinamide (GD), (*S*)-α-(formylamino)propanamide (ADA), and *N*-acetyl-*N*′-methylalaninamide (AD). The dihedral angles, ϕ and ψ, are defined as C(O)−N−C^{α}−C(O) and N−C^{α}−C(O)−N, respectively.

Various quantum mechanical studies on these molecules were performed using Hartree−Fock (HF), density functional theory (DFT), Møller−Plesset (MP2, MP4), and coupled-cluster singles and doubles (CCSD, CCSD(T)) including the local electron correlation methods, because their conformation structure and energy in global or local minimum depend on the level of theory.[2−21] In 1982 Schäfer et al. calculated

* To whom correspondence should be addressed. E-mail: fjtani@labs.fujitsu.com.

10.1021/ct8005437 CCC: $40.75
Published on Web 03/24/2009

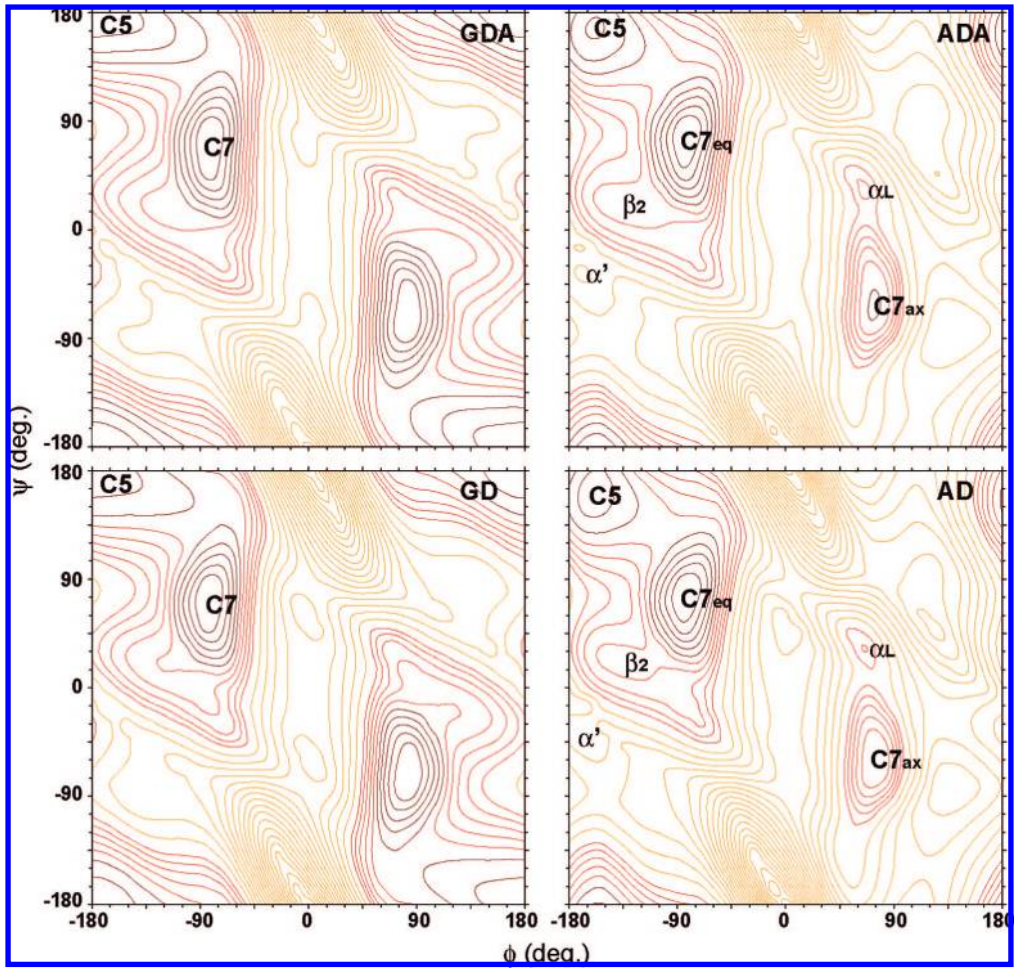

Figure 2. The (ϕ, ψ) maps of GDA, GD, ADA, and AD at the MP2/6-31G(d) level of theory. The maroon contours are drawn every 0.5 kcal/mol from the zero energy to 2.5 kcal/mol. The red contours are drawn every 0.5 kcal/mol from 3 to 5 kcal/mol. The orange contours are drawn every 1 kcal/mol above 6 kcal/mol. The figures were drawn using xfarbe version 2.6c.[34]

low-lying conformers of GD at the HF/4-21 level and concluded that the global minimum was C7 and the second lowest minimum was C5.[3] Using the analogues of GDA and ADA, Head-Gordon et al. obtained the fully relaxed 15° (ϕ, ψ) maps at the HF/3-21G level and then calculated the energies of some stationary points at higher levels of theory.[4] They found that (a) several local minima of GDA and ADA at HF/3-21G disappeared at higher levels, (b) the global minimum of GDA was the C7 conformer at HF/3-21G and MP2/6-31+G(d,p)//HF/6-31+G(d) levels whereas it was the C5 conformer at HF/6-31+G(d), (c) the third lowest local minimum of ADA was the $C7_{ax}$ conformer at HF/3-21G and MP2/6-31+G(d,p)//HF/6-31+G(d) levels whereas it was the β_2 conformer at HF/6-31+G(d). Gould et al. found that the global minimum of GD was C7 at MP2/TZVP//HF/6-31G(d,p) whereas it was C5 at HF/6-31G(d,p) and that the third lowest local minimum of AD was $C7_{ax}$ at MP2/TZVP//HF/6-31G(d,p) whereas it was β_2 at HF/6-31G(d,p).[6]

After these works, higher-level calculations were applied for AD and all gave the same order of the low-lying conformers as $C7_{eq} < C5 < C7_{ax} < \beta_2$.[7,9,12,15,20] Although the relative order of stability was the same at higher level calculations, their structures are significantly different. For example, the equilibrium (ϕ, ψ) angles of the β_2 conformer was (−135.9°, 23.4°) at B3LYP/6-31G(d),[7] but it was (−82.3°, −9.5°) at MP2(Full)/Aug-cc-pVDZ.[12] The hydrogen bond length of N−H···O of the β_2 conformer was 3.51 Å at BLYP/TZVP+ whereas it was 2.95 Å at MP2(Full)/Aug-cc-pVDZ.[12] The first reason for the difficulty to get precise results is the shallow minima and very flat regions of potential energy surfaces with respect to ϕ and ψ. The second is intramolecular hydrogen bonds, and the third is intramolecular dispersive interactions. In addition to these reasons, the artificial energy by intramolecular basis set superposition error (BSSE) makes it more difficult to choose an appropriate level of theory.[11,20,22−25]

In this work, we clarify the accuracy of various levels of quantum mechanical theory by comparing the precise conformation structures and energies of the global and local minima. Because of the accuracy and computational efficiency to calculate rotational energy profiles of ϕ and ψ, we use the density-fitting local coupled-cluster singles and doubles[26,27] with perturbative noniterative local triples[28] at the density-fitting local MP2[26,29,30] geometries with the Aug-cc-pVTZ basis set:[31] DF-LCCSD(T0)/Aug-cc-pVTZ//DF-LMP2/Aug-cc-pVTZ. We compare the ab initio rotational energy profiles with molecular mechanical profiles calculated with AMBER force field variants. Since there are significant

deviations, we optimize the molecular mechanical dihedral parameters of ϕ and ψ to fit the ab initio profiles. Calculations with a local correlation, density-fitting, and CCSD were performed using the MOLPRO package.[32] The other molecular orbital calculations were performed using Gaussian 98.[33] Vibrational frequency analyses at energy minima were performed using both MOLPRO and Gaussian 98. We adopted a frozen core approximation in all molecular orbital calculations.

2. MP2/6-31G(d) Contour Map of (ϕ, ψ)

We first generated the fully relaxed 15° (ϕ,ψ) energy maps of the GDA, GD, ADA, and AD molecules at the MP2/6-31G(d) level of theory in order to clarify the whole energy landscape and obtain the relaxed atomic structure at each (ϕ, ψ) grid point. Figure 2 shows the (ϕ, ψ) maps for GDA, GD, ADA, and AD, which were drawn using xfarbe version 2.6c.[34] For ADA and AD we optimized the molecular structure at the 576 (24 × 24) grid points. For GDA we used the symmetry (ϕ, ψ) =($-\phi$, $-\psi$) and thus 312 GDA structures were optimized. For GD we performed the structure optimization at (ϕ, ψ) and ($-\phi$, $-\psi$) and then symmetrized the (ϕ, ψ) map using the lower energy of the two. These calculations were performed using Gaussian 98 with the default convergence criteria. For each energy minimum conformer we performed vibrational analysis to check the absence of imaginary frequencies at MP2/6-311++G(d,p) for GDA, at MP2/6-31+G(d) for ADA and GD, and at MP2/6-31G(d) for AD.

The contour maps for GD and AD reported by Mackerell et al. are almost the same as ours, except in the vicinity of the α′ conformer of AD.[15] We performed vibrational analysis of the α′ conformer at (−166.1°, −37.2°) to confirm the absence of imaginary frequencies, which is evidence of a local minimum.

Global and local minima are clarified by the (ϕ, ψ) contour maps obtained at the MP2/6-31G(d) level, but their precise energies and structures depend on the level of theory. We first apply various levels of theory to the smallest molecule of GDA to examine the accuracy of the method, including MP2, MP4, CCSD with or without the local correlation method, and the density fitting approximation (DF). We use not only Pople basis sets like 6-311++G(d,p) but also augmented correlation consistent Dunning basis sets like Aug-cc-pVnZ (n = D, T, Q). DF reduces the calculation cost of two-electron-four-index integrals by several times.

3. Comparison of Levels of Theory

When optimizing the geometries of conformers, i.e., local minima, using MOLPRO and Gaussian 98, we adopted a tight convergence criteria in that the maximum force is 1.5 × 10^{-5}, the rms force is 1 × 10^{-5}, the maximum displacement is 6 × 10^{-5}, and the rms displacement is 4 × 10^{-5} atomic units. This corresponds to the "Opt=Tight" keyword of Gaussian 98.

For MOLPRO, we tightened the SCF convergence criterion on density matrix to 10^{-8} by specifying "accu=16". In the local calculation, the two most diffuse functions of each angular momentum functions were ignored in the localization to yield better-localized orbitals; unless otherwise noted, completion criterion of 0.99 was used for the orbital domain selection by specifying "PMDEL=2" and "THRBP=0.99", respectively. When computing the extrapolation to the complete basis set (CBS) limit, we employed the $E_X = E_{CBS} + AX^{-3}$ formula[35] using the Aug-cc-pVTZ and Aug-cc-pVQZ basis sets.

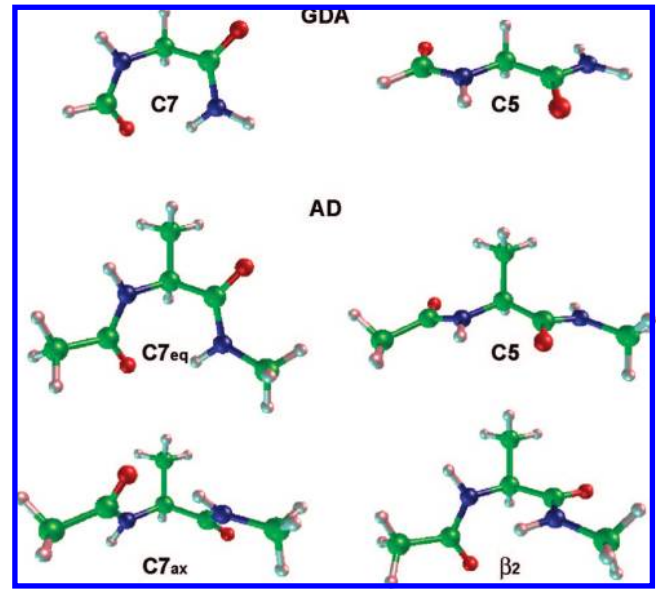

Figure 3. Graphical representations of low-lying conformers for GDA and AD optimized at the DF-LMP2/Aug-cc-pVTZ level of theory. The figures were drawn using xmo V4.0.[36]

Table 1. Torsional Angles ϕ and ψ and N−H···O Hydrogen Bond Length r of C7 and C5 Conformers of GDA Calculated at Different Levels of Theory[a]

	C7			C5		
theory	ϕ	ψ	r	ϕ	ψ	r
HF/6-31G(d)	−84.9	68.1	2.22	180.0	180.0	2.21
HF/6-31+G(d)[b]	−85.3	67.3	2.24	180.0	180.0	2.22
MP2/6-31G(d)	−82.5	74.2	2.08	175.7	179.5	2.17
MP2/6-31+G(d)	−82.5	74.7	2.10	169.3	173.7	2.20
MP2/6-31++G(d,p)	−82.8	72.4	2.09	162.4	177.7	2.20
MP2/6-311++G(d,p)	−82.1	76.7	2.10	165.8	171.6	2.21
MP2/AVDZ	−82.4	68.0	2.06	180.0	180.0	2.20
MP2/AVTZ	−82.6	67.4	2.04	180.0	180.0	2.18
LMP2/AVTZ	−82.8	68.5	2.08	180.0	180.0	2.19
DF-LMP2/AVTZ	−82.8	68.5	2.08	180.0	180.0	2.19

[a] Angles are in degrees, and hydrogen bond length is in angstroms. [b] The (ϕ, ψ) is (−85.2, 67.4) for C7 conformer and (180.0, 180.0) for C5 conformer in ref 4 which does not report the hydrogen bond lengths.

Figure 3 shows low-lying conformers of GDA and AD molecules which were drawn using the xmo V4.0 MO visualizer.[36]

GDA. We examined the precise structures of the C7 and C5 conformers of GDA at different levels of theory. The C7 and C5 conformers have different N−H···O hydrogen bonds (Figure 3). Their bond length and torsional angles of ϕ and ψ are listed in Table 1. We abbreviate the basis sets of Aug-cc-pVDZ, Aug-cc-pVTZ, and Aug-cc-pVQZ as AVDZ, AVTZ, and AVQZ, respectively. The ϕ and ψ of

Table 2. Relative Energies (kcal/mol) of C7 and C5 Conformers of GDA Calculated at Different Levels of Theory

theory	C7	C5
HF/6-31G(d)	0.45	0.00
HF/6-31+G(d)[a]	0.58	0.00
MP2/6-31G(d)	0.00	1.23
MP2/6-31+G(d)	0.00	1.37
MP2/6-31++G(d,p)	0.00	1.35
MP2/6-311++G(d,p)	0.00	1.08
MP4/6-311G(d,p)//MP2/6-31G(d)	0.00	1.52
MP4/6-311+G(d,p)//MP2/6-31G(d)	0.00	1.53
MP4/6-311++G(d,p)//MP2/6-31G(d)	0.00	1.56
MP4/6-311+G(d,p)//MP2/6-31+G(d)	0.00	1.29
MP4/6-311++G(d,p)//MP2/6-31++G(d,p)	0.00	1.24
MP2/AVDZ	0.00	1.03
MP2/AVTZ//MP2/AVDZ	0.00	0.75
MP2/AVTZ	0.00	0.74
MP2/AVTZ//LMP2/AVTZ	0.00	0.73
DF-MP2/AVTZ//DF-LMP2/AVTZ	0.00	0.73
LMP2/AVTZ	0.00	0.51
DF-LMP2/AVTZ	0.00	0.51
LMP4/AVTZ//LMP2/AVTZ	0.00	0.44
DF-LMP4/AVTZ//DF-LMP2/AVTZ	0.00	0.44
CCSD(T)/AVTZ//MP2/AVTZ	0.00	0.78
CCSD(T)/AVTZ//LMP2/AVTZ	0.00	0.77
LCCSD(T0)/AVTZ//LMP2/AVTZ	0.00	0.44
DF-LCCSD(T0)/AVTZ//DF-LMP2/AVTZ	0.00	0.44

[a] The value is the same as in ref 4.

the C5 conformer are all 180° at the MP2, LMP2, and DF-LMP2 levels with Dunning basis set, but they deviate from 180° at MP2 with Pople basis sets. The deviation of ϕ is about 18° at MP2/6-31++G(d,p), about 14° at MP2/6-311++G(d,p), and about 4° at MP2/6-31G(d). Larger Pople basis sets gave larger deviation in Table 1. Similar deviations are observed in the ψ values of the C7 conformer while the deviations are smaller.

The intermolecular BSSE effects on geometry and interaction energy can be accounted for by using the counterpoise procedure. Schütz et al. reported that the interaction energy and O−O distance of water dimer at the MP2/AVTZ level were −5.18 kcal/mol and 2.907 Å, that the counterpoise corrected values were −4.72 kcal/mol and 2.932 Å, and those at DF-LMP2/AVTZ were −4.67 kcal/mol and 2.935 Å, respectively.[29] Although there is no straightforward way to correct for intramolecular BSSE, it is well-known that the local correlation method reduces the intramolecular BSSE.[25]

Since the N−H···O hydrogen bond of the C7 conformer is stronger than that of the C5 conformer, the hydrogen bond length of the C7 conformer ranges from 2.04 to 2.24 Å depending on the basis set, while that of the C5 conformer ranges from 2.17 Å to 2.22 Å. The HF calculation gave a little longer hydrogen bond lengths for both C5 and C7 conformers, as it does not take into account both dispersion and electron correlation. The hydrogen bond length at MP2/AVTZ is the shortest of all and is 0.04 Å shorter than that at DF-LMP2/AVTZ. This is consistent with the BSSE correction which slightly extended the O−O distance of water dimer.

Table 2 lists the relative energies of the C7 and C5 conformers of GDA at various levels of theory. All the relative energies at the MP2 and MP4 levels with Pople basis sets are larger than those with Dunning basis sets. Pople basis sets cannot give precise structures and relative energies of the C7 and C5 conformers and they are not suitable for investigating precise energy profiles of the protein model system. Within Dunning basis sets, the relative energy varies more than 0.5 kcal/mol depending on the level of theory. Canonical MP2 and CCSD(T) give slightly larger relative energies than those at the local correlation methods of LMP2 and LCCSD(T0), because the canonical methods give BSSE excessive lower energies to the hydrogen bond of the C7 conformer. There is no difference in structure between DF-LMP2/AVTZ and LMP2/AVTZ in Table 1, and there is no difference in relative energy in Table 2 by the density fitting approximation (DF). We did not observe any deviation owing to DF in our calculations. DF is very useful for reducing the calculation cost.

Table 3. The Relative Energies (kcal/mol) of C5 Conformer to C7 Conformer of GDA Calculated at the DF-LMP2/AVTZ and MP2/AVTZ Geometries

	geometry	
energy	DF-LMP2/AVTZ	MP2/AVTZ
MP2/AVTZ	0.73	0.74
DF-MP2/AVTZ	0.73	−
DF-MP2/AVQZ	0.64	−
DF-MP2/CBS	0.59	−
DF-LMP2/AVTZ	0.51	0.50
DF-LMP2/AVQZ[a]	0.54	−
DF-LMP2/CBS	0.56	−
DF-LMP4/AVTZ	0.44	0.42
CCSD(T)/AVTZ	0.77	0.78
DF-LCCSD(T0)/AVTZ	0.44	0.41
DF-LCCSD(T0)/AVQZ[a]	0.46	−
DF-LCCSD(T0)/CBS	0.48	−

[a] THRBP = 0.993 for C7 conformer, and THRBP = 0.992 for C5 conformer.

We examined the basis set truncation error (BSTE) by enlarging the basis set. Table 3 lists the relative energies of the C5 conformer to the C7 conformer calculated at the DF-LMP2/AVTZ and MP2/AVTZ geometries. The relative energies only depend on the level of theory used in the energy calculation, and the differences between them when comparing the DF-LMP2 and MP2 geometries are negligible. When the basis set is enlarged from AVTZ to CBS, the relative energy at the canonical DF-MP2 decreases while one at the local correlation DF-LMP2 increases, because the former contains both BSTE and BSSE while the latter contains only BSTE. We evaluate the BSSE at DF-MP2/AVTZ as 0.19 = (0.73 − 0.59) − (0.51 − 0.56) in kcal/mol. It decreases when the basis set is enlarged. On the reasonable assumption that DF-LCCSD(T0)/AVTZ//DF-LMP2/AVTZ is essentially free from BSSE, we calculate the BSTE in the relative energy between the C5 and C7 conformers as being 0.04 kcal/mol.

AD. AD is the largest molecule in this study. Table 4 lists the torsional angles, ϕ and ψ, and the hydrogen bond lengths of N−H···O for the $C7_{eq}$, C5, $C7_{ax}$, and β_2 conformers of AD at different levels of theory including several reported values.[7,9,12,15] The graphical representations for these conformers at DF-LMP2/AVTZ are shown in Figure 3. The structures of the $C7_{eq}$, C5, and $C7_{ax}$ conformers are not sensitive to the level of theory, but the β_2 conformer is

Table 4. The Torsional Angles, ϕ and ψ, and the Hydrogen Bond Lengths r of N−H···O for $C7_{eq}$, C5, $C7_{ax}$, and β_2 Conformers of AD at Different Levels of Theory[a]

	$C7_{eq}$			C5			$C7_{ax}$			β_2		
theory	ϕ	ψ	r	ϕ	ψ	r	ϕ	ψ	r	ϕ	ψ	r
HF/6-31G(d)	−85.4	79.3	2.23	−157.3	158.8	2.22	75.9	−55.7	2.04	−132.6	22.4	3.66
HF/6-31+G(d)	−86.4	79.4	2.26	−153.8	151.9	2.24	75.9	−56.4	2.05	−102.7	4.1	3.28
HF/VDZ	−84.7	81.0	2.23	−155.6	162.7	2.20	75.7	−66.9	2.04	−138.1	25.0	3.72
HF/AVDZ	−86.1	80.9	2.26	−155.6	156.5	2.25	75.8	−53.8	2.04	−99.4	1.8	3.21
B3LYP/6-31G(d)	−82.9	72.9	2.04	−158.1	164.1	2.15	73.6	−57.7	1.92	−126.7	20.9	3.56
B3LYP/6-31G(d)	−81.9	72.3	−	−157.3	165.3	−	73.8	−60.0	−	−135.9	23.4	−
B3LYP/6-31+G(d)	−83.1	74.8	2.08	−155.2	159.1	2.21	73.1	−55.5	1.94	−113.4	12.6	3.40
MP2/6-31G(d)	−83.1	77.8	2.06	−158.4	161.3	2.17	74.4	−64.1	1.93	−137.9	22.9	3.71
MP2/6-31+G(d)	−82.2	79.7	2.09	−153.8	151.9	2.26	74.5	−55.9	1.93	−89.0	−5.3	3.04
MP2/6-31++G(d,p)	−82.4	80.4	2.09	−152.9	151.5	2.27	74.7	−55.9	1.92	−91.8	−3.6	3.08
MP2/6-311++G(d,p)[e]	−81.9	81.6	2.09	−158.4	151.6	2.28	74.3	−57.4	1.91	−90.7	−7.8	3.12
MP2(Full)/AVDZ	−82.6	75.8	2.02	−161.1	155.5	2.23	73.7	−53.7	1.88	−82.3	−9.5	2.95
DF-LMP2/AVTZ	−83.1	75.0	2.05	−159.1	161.7	2.19	73.7	−53.2	1.90	−88.1	−4.6	3.02

[a] Angles are in degrees, and hydrogen bond lengths are in angstroms. [b] Total energies in hartree: $C7_{eq}$ = −495.855 139 7, C5 = −495.852 890 7, $C7_{ax}$ = −495.850 994 3, β_2 = −495.850 199 2. [c] Hydrogen bond lengths are not reported in ref 7. [d] Calculated angles in refs 9 and 15, and this work agrees within a 0.3° range. Hydrogen bond lengths are not reported in the references. [e] Calculated angles in ref 15, and this work agrees within a 0.1° range. Hydrogen bond lengths are not reported in the references. [f] Reference 12.

Table 5. Relative Energies (kcal/mol) of $C7_{eq}$, C5, $C7_{ax}$, and β_2 Conformers of AD Calculated at Different Levels of Theory

theory	$C7_{eq}$	C5	$C7_{ax}$	β_2
HF/6-31G(d)	0.0	0.41	2.82	2.58
HF/6-31+G(d)	0.0	0.30	2.87	2.42
HF/VDZ	0.0	0.54	3.07	2.35
HF/AVDZ	0.0	0.21	2.93	2.55
B3LYP/6-31G(d)	0.0	1.41	2.60	3.10
B3LYP/6-31G(d)[a]	0.0	1.43	2.61	3.18
B3LYP/6-31+G(d)	0.0	1.09	2.49	2.74
MP2/6-31G(d)[b]	0.0	1.73	2.54	3.30
MP2/6-31+G(d)	0.0	1.79	2.42	2.98
MP2/6-31++G(d,p)	0.0	1.68	2.18	2.91
MP2/6-311++G(d,p)[c]	0.0	1.66	2.33	2.83
MP2(Full)/AVDZ[d]	0.0	1.91	2.28	3.11
MP2(Full)/CBS//MP2(Full)/AVDZ[d]	0.0	1.39	2.66	3.35
LMP2/VQZ(-g)//MP2/6-311++G(d,p)[e]	0.0	0.91	2.06	2.51
MP4/6-311G(d,p)//MP2/6-31G(d)	0.0	1.88	2.68	2.87
MP4-BSSE/VTZ(-f)//MP2/6-31G(d)[f]	0.0	0.89	2.55	2.56
CCSD(T)/CBS-MP2//MP2/AVDZ[g]	0.0	1.43	2.41	3.23
DF-MP2/AVTZ//DF-LMP2/AVTZ	0.0	1.46	2.29	3.04
DF-MP2/AVQZ//DF-LMP2/AVTZ	0.0	1.36	2.36	3.08
DF-MP2/CBS//DF-LMP2/AVTZ	0.0	1.32	2.39	3.12
DF-LMP2/AVTZ	0.0	1.22	2.41	2.86
DF-LMP2/AVQZ//DF-LMP2/AVTZ[h]	0.0	1.24	2.44	2.99
DF-LMP2/CBS//DF-LMP2/AVTZ	0.0	1.28	2.44	3.09
DF-LMP4/AVTZ//DF-LMP2/AVTZ	0.0	1.16	2.43	2.65
DF-LCCSD(T0)/AVTZ//DF-LMP2/AVTZ	0.0	1.14	2.38	2.71
DF-LCCSD(T0)/AVQZ//DF-LMP2/AVTZ[h]	0.0	1.19	2.41	2.87
DF-LCCSD(T0)/CBS//DF-LMP2/AVTZ	0.0	1.24	2.42	3.00

[a] Reference 7. [b] Calculated relative energies in ref 15, and this work agrees within a 0.02 kcal/mol range. [c] Calculated relative energies in this work are identical with those in ref 15. [d] Reference 12. [e] Reference 15. [f] Reference 9. [g] Reference 20. [h] THRBP = 0.992.

sensitive because it is located in the very flat region of the potential energy surface.[12]

Table 5 lists the relative energies for the $C7_{eq}$, C5, $C7_{ax}$, and β_2 conformers of AD at different levels of theory including several reported values.[7,9,12,15,20] There are the same features as those of GDA. The results at the HF levels are qualitatively inconsistent with those at higher levels of theory. All the energies of the C5 conformer at the MP2 levels with Pople basis sets are larger than those with Dunning basis sets. Because of BSSE, the canonical DF-MP2 calculations give larger energies for the C5 conformer than the local correlation DF-LMP2 calculations. Enlarging the basis sets from AVTZ to CBS, the DF-MP2 energy of the C5 conformer decreases while its DF-LMP2 energy increases.

For DF-LCCSD(T0), the energy differences between AVTZ and CBS are less than 0.3 kcal/mol for all the low-lying conformers. Taking into account computational cost and accuracy of the theory, DF-LCCSD(T0)/AVTZ//DF-LMP2/AVTZ is the best choice for calculating the torsional energy profiles of ϕ and ψ.

Low-Lying Conformation. Table 6 lists the structures and relative energies of the low-lying conformers of GDA, GD, ADA, and AD at DF-LCCSD(T0)/AVTZ//DF-LMP2/AVTZ. Kaminský and Jensen calculated the conformation structures and relative energies of some peptides, including GD and AD, at their CCSD(T)/CBS-MP2//MP2/AVDZ method which extrapolates the energy to the complete basis set limit with the HF/cc-pVXZ, MP2/cc-pVXZ (X = D, T, and Q), and the CCSD(T)/cc-pVDZ energies, and then compared them with molecular mechanical energies using various force fields.[20] As they pointed out, there are some discrepancies between the ab initio results and molecular mechanics results. We try to improve the molecular mechanical force field parameters by comparing the torsional energy profiles of ϕ and ψ.

4. Torsional Energy Profiles

4.1. Quantum Mechanical Torsional Profile. First we looked for the lowest energy path for ϕ (or ψ) to change from −180° to 180° in the contour map (Figure 2). Using the lowest mesh point structure as an initial structure, we fully optimized the molecular structure by the MP2/6-31G(d) calculation with fixed ϕ (or ψ) at the 15° step mesh value and then performed the MP4/6-311G(d,p) energy calculation to get a rotational energy profile of ϕ (or ψ). The torsional

Table 6. Structures and Relative Energies of Low-Lying Conformers of GDA, GD, ADA, and AD Calculated at the DF-LCCSD(T0)/Aug-cc-pVTZ//DF-LMP2/Aug-cc-pVTZ Level[a]

	C7/C7$_{eq}$				C5				C7$_{ax}$				β_2			
	ϕ	ψ	r	E	ϕ	ψ	r	E	ϕ	ψ	r	E	ϕ	ψ	r	E
GDA	−82.8	68.5	2.08	0.0	180.0	180.0	2.19	0.44								
GD	−82.8	70.6	2.05	0.0	180.0	180.0	2.18	0.91[b]								
ADA	−83.2	73.5	2.08	0.0	−159.8	165.1	2.19	0.85	73.5	−52.5	1.95	2.16	−90.0	−2.2	3.06	2.65
AD	−83.1	75.0	2.05	0.0	−159.1	161.7	2.19	1.14	73.7	−53.2	1.90	2.38	−88.1	−4.6	3.02	2.71

[a] Angles are in degrees and hydrogen bond lengths (N−H···O) are in angstroms. Relative energy with respect to C7 or C7$_{eq}$ in kcal/mol. C7 or C7$_{eq}$ energies of GDA, GD, ADA, and AD are −377.358 480 3, −455.842 733 4, −416.604 581 2, and −495.088 760 7 hartree, respectively. [b] Relative energy at CCSD(T)/CBS-MP2//MP2/Aug-cc-pVDZ is 0.98 kcal/mol.[20]

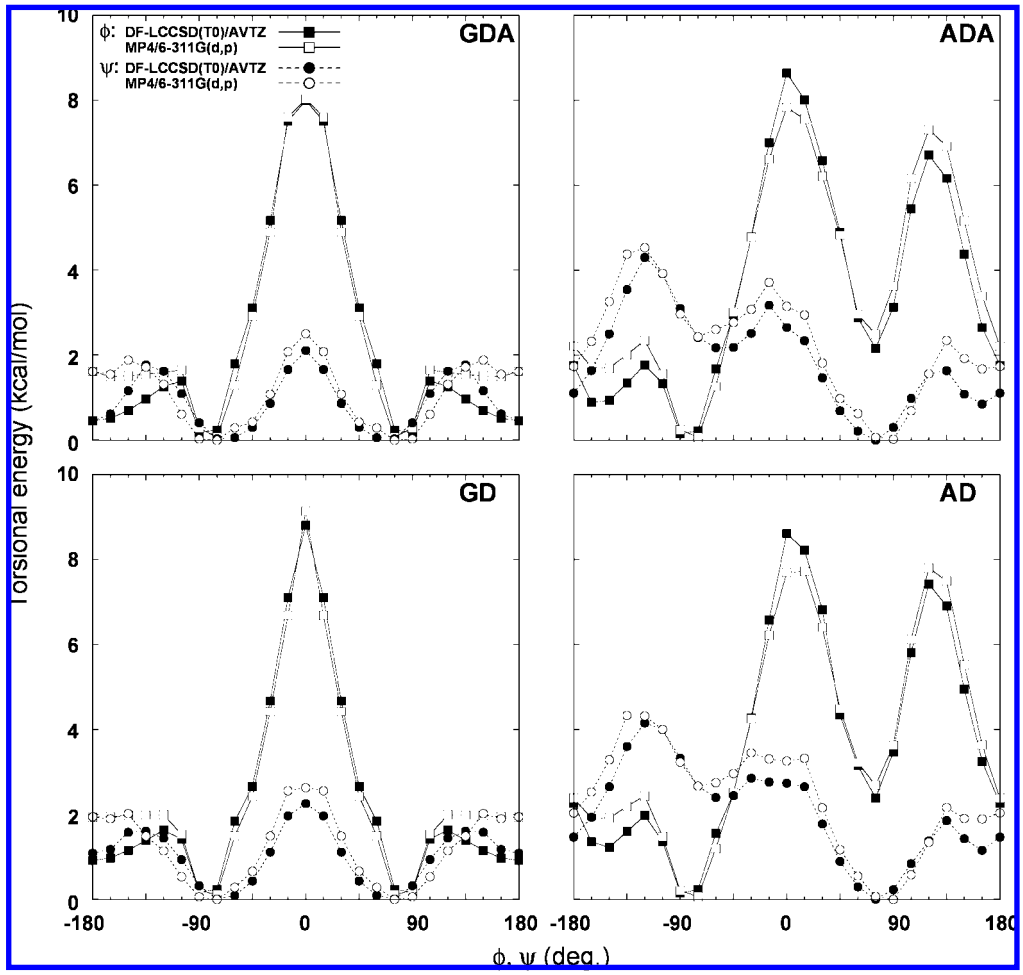

Figure 4. The torsional energy profiles of ϕ and ψ of GDA, GD, ADA, and AD. The solid lines are the ϕ profiles and the dashed lines are the ψ profiles. The filled squares and filled circles are at the DF-LCCSD(T0)/Aug-cc-pVTZ//DF-LMP2/Aug-cc-pVTZ level and the open squares and open circles are at the MP4/6-311G(d,p)//MP2/6-31G(d) level.

energy profile at the MP4/6-311G(d,p)//MP2/6-31G(d) level was used in the development of general AMBER force field (GAFF).[37]

Starting from the optimized MP2/6-31G(d) structure at the 15° step, we fully optimized the molecular structure by DF-LMP2/AVTZ with the fixed ϕ (or ψ) value using the default convergence criteria of structure optimization by MOLPRO and then calculated more accurate energy at the DF-LCCSD(T0)/AVTZ level to get a rotational energy profile of ϕ (or ψ) at DF-LCCSD(T0)/AVTZ//DF-LMP2/AVTZ. In the previous section we note the differences between MP2/6-31G(d) and DF-LMP2/AVTZ in the molecular structures and energies of the low-lying conformers, but they are smaller differences from the viewpoint of the whole (ϕ, ψ) contour maps. In addition, we performed the vibrational analysis for the low-lying conformers at the DF-LMP2/AVTZ level of theory to confirm the absence of imaginary frequencies. Therefore, it can be safely assumed that the energy minimum character is preserved in the torsional energy profiles at DF-LCCSD(T0)/AVTZ//DF-LMP2/AVTZ.

Figure 4 shows the torsional energy profiles for GDA, GD, ADA, and AD. For GDA and GD, the profiles of both ϕ and ψ from 105° to 180° disagree between DF-LCCSD(T0) and MP4. Especially there are significant differences in the vicinity of 180°, which is close to the C5 conformer. The profiles at DF-LCCSD(T0) indicate that a local minimum is

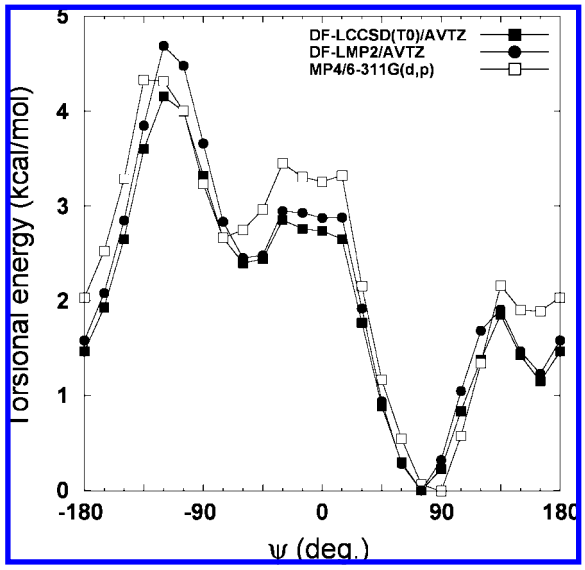

Figure 5. The torsional energy profiles of ψ of AD. The filled squares are at DF-LCCSD(T0)/Aug-cc-pVTZ, and the filled circles are at DF-LMP2/Aug-cc-pVTZ with the same geometries at DF-LMP2/Aug-cc-pVTZ. The open squares are at MP4/6-311G(d,p)//MP2/6-31G(d).

at 180° unlike those at MP4. The MP4 torsional energy at 180° is almost twice that at DF-LCCSD(T0) for GD, and it is three times larger for GDA. For ADA and AD, not only the energy value but also the position of a local minimum or maximum differ between DF-LCCSD(T0) and MP4, like in the vicinity of $\psi = -60°$ and $-135°$.

Figure 5 shows that the torsional energy profile of ψ of AD at the DF-LCCSD(T0)/AVTZ and DF-LMP2/AVTZ levels of theory with the same geometry at DF-LMP2/AVTZ, together with the profile at MP4/6-311G(d,p)//MP2/6-31G(d). There is a significant difference between DF-LCCSD(T0) and DF-LMP2 around $-120°$. This difference is more than 0.5 kcal/mol. Similar differences between DF-LCCSD(T0) and DF-LMP2 were also observed in other torsional profiles. Although the DF-LMP2 profile better agrees with the DF-LCCSD(T0) profile than the MP4/6-311G(d,p) profile, the higher-order correlation beyond MP2 is significant for some conformers with higher energies.

4.2. Molecular Mechanical Torsional Profile. The total energy in the AMBER force field model is given by[1]

$$E_{\text{total}} = \sum_{\text{bonds}} K_r(r_{ij} - r_{\text{eq}})^2 + \sum_{\text{angles}} K_\theta(\theta_{ijk} - \theta_{\text{eq}})^2 + \sum_{\text{dihedrals}} \sum_n \frac{V_n}{2}[1 + \cos(n\varphi_{ijkl} - \gamma_n)] + \sum_{i<j} \left[4\varepsilon_{ij}\left(\left(\frac{\sigma_{ij}}{r_{ij}}\right)^{12} - \left(\frac{\sigma_{ij}}{r_{ij}}\right)^{6}\right) + \frac{q_i q_j}{r_{ij}} \right] \quad (1)$$

Here, r_{eq} and θ_{eq} are equilibrium structural parameters; K_r, K_θ, V_n are force constants; n is multiplicity, and γ_n is the phase angle for the torsional angle parameters. ε_{ij} and σ_{ij} are van der Waals parameters, and q_i is the partial charge.

We compare the torsional energy profiles of ϕ and ψ between the DF-LCCSD(T0)/AVTZ//DF-LMP2/AVTZ level of theory and molecular mechanics with AMBER force field variants. In order to derive the molecular mechanical torsional profiles, we used version 3.3.3 of the GROMACS molecular dynamics suite[38] and the AMBER force field variants ported to GROMACS by Sorin and Pande.[39] As the initial structure for the molecular mechanical calculation, we used the 15° step structure optimized by DF-LMP2/AVTZ and performed an energy minimization by GROMACS with the fixed ϕ (or ψ) value to get a torsional energy profile.

Figure 6 shows the molecular mechanical profiles with the ab initio profiles. In the GD profiles, the potential barrier from the C7 conformer to the C5 conformer is too large in all molecular mechanical force fields. The lowest energy structure in AMBER99 (f99) is the C5 conformer, not the C7 conformer, and the molecular mechanical ψ values of the C7 conformer largely deviate from the ab initio value (Table 6). For AD, the peak around $-120°$ in the ψ profile is too large in all the molecular mechanical force fields and AMBER99SB (f99sb)[40] has a too large barrier around 120° in the ϕ profile. We suppose these deviations are one of the reasons why the molecular dynamics simulation with AMBER force fields did not have a good agreement with the experiments.[39]

A force field formulator for organic molecules (FF-FOM) was developed to assign force field parameters to arbitrary organic molecules in a unified manner including proteins and nucleic acids.[41] FF-FOM uses the GAFF bond parameters which have much improved characters after the experience of the AMBER99 force field parametrization.[42] The GROMACS input files of the unified force field for all amino acids and nucleic acids including GD and AD are available as a Supporting Information of ref 41. It uses the AMBER restrained electrostatic potential charges (RESP) and van der Waals potential parameters,[1] and the GAFF bond, angle, and dihedral parameters.[37]

Since GAFF has the same dihedral parameters for protein backbone torsions as AMBER99, we optimized the backbone dihedral parameters in order to get a better agreement with the ab initio profiles using the unified force field for GD and AD. Without any modification of other force field parameters, we first optimized the dihedral parameters of C−N−C$^\alpha$−C (ϕ) and N−C$^\alpha$−C−N (ψ) comparing the ab initio and molecular mechanical torsional profiles of GD. Then, using the obtained dihedral parameters of ϕ and ψ, we optimized the side-chain-related dihedral parameters of C−N−C$^\alpha$−C$^\beta$ (ϕ') and N−C−C$^\alpha$−C$^\beta$ (ψ'), comparing the torsional profiles of AD. In the optimization, we performed an exhaustive grid search in the parameter space of four amplitudes (V_1, V_2, V_3, V_4) and four phases (γ_1, γ_2, γ_3, γ_4) using the maximum absolute error function defined as

$$\text{MAE} = \max_{i<j} |E^i_{\text{QM}}(j) - E^i_{\text{MM}}(j)| \quad (2)$$

where $E^i_{\text{QM}}(j)$ is the ab initio energy of conformer j with conformer i as a reference, and $E^i_{\text{MM}}(j)$ is the molecular mechanical energy of conformer j with conformer i as a reference.[40] Amplitudes were checked from 0 to 3 kcal/mol, and phases were set to either 0 or π radians.

Table 7 lists the optimized dihedral parameters, and Figure 7 compares the optimized molecular mechanical profiles with

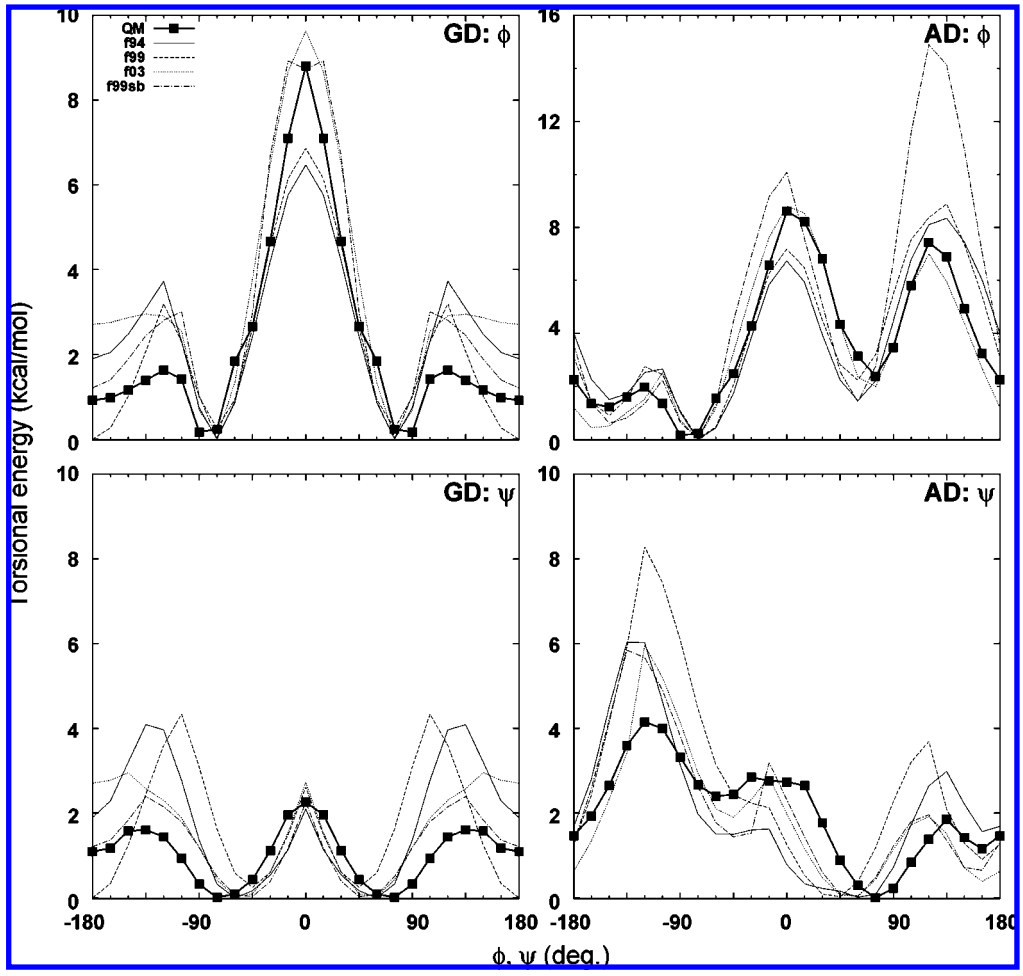

Figure 6. The torsional energy profiles of ϕ and ψ calculated with four AMBER force field variants (f94, f99, f03, f99sb) for GD and AD. The filled squares with a solid line show the torsional energy profile of ϕ and ψ at the DF-LCCSD(T0)/Aug-cc-pVTZ//DF-LMP2/Aug-cc-pVTZ level.

Table 7. Optimized Molecular Mechanical Dihedral Parameters for the Protein Backbone Torsions[a]

		V_1	γ_1	V_2	γ_2	V_3	γ_3	V_4	γ_4
ϕ	C−N−C$^\alpha$−C	0.17	0	0.21	0	0.07	π	0.10	0
ψ	N−C$^\alpha$−C−N	0.15	0	0.93	π	0.77	π	0.39	π
ϕ'	C−N−C$^\alpha$−C$^\beta$	0.25	π	0.19	π	0.13	π	0.14	π
ψ'	N−C−C$^\alpha$−C$^\beta$	0.48	π	0.39	π	0.30	0	0.33	π

[a] Phases are in radians, and amplitudes are in kcal/mol.

the ab initio profiles. We optimized only the dihedral parameters of the four torsions without any modification of other parameters. Our optimized profiles agree with the ab initio profiles much better than with the AMBER force field variants, but there are small deviations caused by other (general) AMBER parameters. Figure 8 compares the molecular structure of the $C7_{eq}$ conformer of AD between the DF-LMP2/AVTZ and molecular mechanical calculations. The molecular mechanical (MM) structure reasonably agrees with the ab initio (QM) structure, but the hydrogen bonds in the terminal methyl have slightly different orientations. The same deviation was observed in the GD and AD structures with the AMBER force field variants. This is an example of a remaining issue that needs to be overcome to improve the "minimalist model" of eq 1, although the protein does not have a methyl at either terminal in a standard condition. Our optimized dihedral parameters for the protein backbone torsions significantly differ from those of the AMBER force field variants. We hope the new dihedral parameters will improve the accuracy of molecular dynamics simulations for protein folding and absolute binding free energies.

5. Conclusion

In order to determine the starting geometry to get the fully relaxed torsional energy profiles of ϕ and ψ, we first generated the fully relaxed 15° (ϕ, ψ) maps of GDA, GD, ADA, and AD at the MP2/6-31G(d) level of theory. Global and local minimum conformers were clarified from the (ϕ, ψ) contour maps, but their precise energies and structures depend on the level of theory. Comparing low-lying conformers of GDA and AD at different levels of theory, we concluded that DF-LCCSD(T0)/Aug-cc-pVTZ//DF-LMP2/Aug-cc-pVTZ is the best choice for calculating the torsional energy profiles. It excludes the intramolecular BSSE and gives accurate energies with BSTE less than 0.3 kcal/mol.

Finding out the lowest energy path for ϕ (or ψ) to change from −180 to 180 degrees in the contour map, we performed

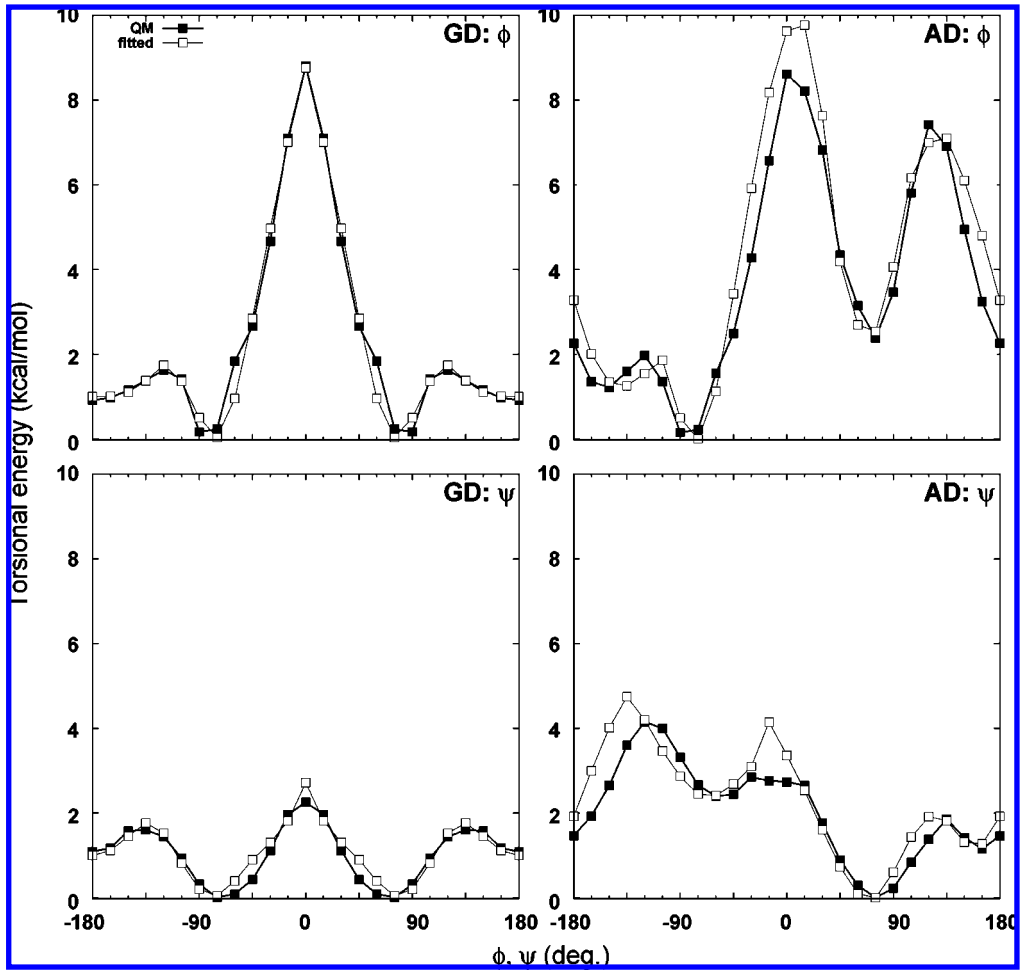

Figure 7. The molecular mechanical torsional energy profiles of GD and AD calculated with the optimized dihedral parameters. The filled squares show the torsional energy profile at the DF-LCCSD(T0)/Aug-cc-pVTZ//DF-LMP2/Aug-cc-pVTZ level, and the open squares show the optimized molecular mechanical profile.

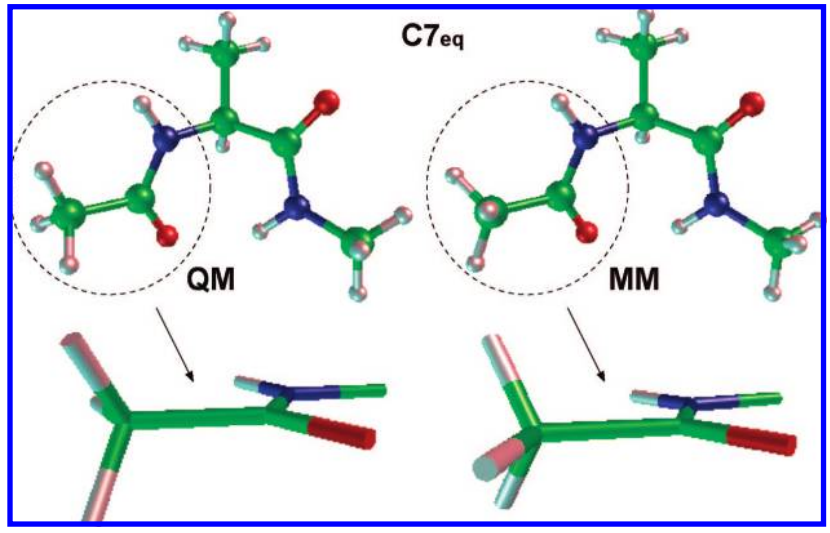

Figure 8. Molecular structures of the $C7_{eq}$ conformer of AD. The QM structure was obtained by the DF-LMP2/Aug-cc-pVTZ level of theory and the MM structure was obtained by the molecular mechanical calculation with our optimized dihedral parameters. The figures were drawn using xmo V4.0.[36]

a DF-LCCSD(T0)/Aug-cc-pVTZ//DF-LMP2/Aug-cc-pVTZ level calculation to get the torsional energy profiles of ϕ and ψ. Molecular mechanics with the AMBER force field variants gave significantly different torsional profiles, so we optimized the molecular mechanical dihedral parameters of the protein backbone to fit the ab initio torsional profiles. We hope the optimized dihedral parameters will improve the accuracy of molecular dynamics simulations.

Supporting Information Available: Optimized geometries and total energies at the DF-LCCSD(T0)/Aug-cc-pVTZ//DF-LMP2/Aug-cc-pVTZ level in the torsional energy profiles of ϕ and ψ are available free of charge via the Internet at http://pubs.acs.org.

References

(1) Cornell, W. D.; Cieplak, P.; Bayly, C. I.; Gould, I. R.; Merz, K. M., Jr.; Ferguson, D. M.; Spellmeyer, D. C.; Fox, T.; Caldwell, J. W.; Kollman, P. A. *J. Am. Chem. Soc.* **1995**, *117*, 5179–5197.

(2) Pullman, B.; Pullman, A. *Adv. Protein Chem.* **1974**, *28*, 347–526.

(3) Schäfer, L.; van Alsenoy, C.; Scarsdale, J. N. *J. Chem. Phys.* **1982**, *76*, 1439–1444.

(4) Head-Gordon, T.; Head-Gordon, M.; Frisch, M. J.; Brooks, C. L., III; Pople, J. A. *J. Am. Chem. Soc.* **1991**, *113*, 5989–5997.

(5) Shang, H. S.; Head-Gordon, T. *J. Am. Chem. Soc.* **1994**, *116*, 1528–1532.

(6) Gould, I. R.; Cornell, W. D.; Hiller, I. H. *J. Am. Chem. Soc.* **1994**, *116*, 9250–9256.

(7) Jalkanen, K. J.; Suhai, S. *Chem. Phys.* **1996**, *208*, 81–116.

(8) Cornell, W. D.; Gould, I. R.; Kollman, P. A. *J. Mol. Struct. (THEOCHEM)* **1997**, *392*, 101–109.

(9) Beachy, M. D.; Chasman, D.; Murphy, R. B.; Halgren, T. A.; Friesner, R. A. *J. Am. Chem. Soc.* **1997**, *119*, 5908–5920.

(10) Rodríguez, A. M.; Baldoni, H. A.; Suvire, F.; Vázquez, R. N.; Zamarbide, G.; Enriz, R. D.; Farkas, Ö.; Perczel, A.; McAllister, M. A.; Torday, L. L.; Papp, J. G.; Csizmadia, I. G. *J. Mol. Struct. (THEOCHEM)* **1998**, *455*, 275–301.

(11) Yu, C.-H.; Norman, M. A.; Schäfer, L.; Ramek, M.; Peeters, A.; van Alsenoy, C. *J. Mol. Struct.* **2001**, *567−568*, 361–374.

(12) Vargas, R.; Garza, J.; Hay, B. P.; Dixon, D. A. *J. Phys. Chem. A* **2002**, *106*, 3213–3218.

(13) Perczel, A.; Farkas, Ö.; Jákli, I.; Topol, I. A.; Csizmadia, I. G. *J. Comput. Chem.* **2003**, *24*, 1026–1042.

(14) Duan, Y.; Wu, C.; Chowdhury, S.; Lee, M. C.; Xiong, G.; Zhang, W.; Yang, R.; Cieplak, P.; Luo, R.; Lee, T.; Caldwell, J.; Wang, J.; Kollman, P. *J. Comput. Chem.* **2003**, *24*, 1999–2012.

(15) Mackerell, A. D., Jr.; Feig, M.; Brooks, C. L., III. *J. Comput. Chem.* **2004**, *25*, 1400–1415.

(16) Papamokos, G. V.; Demetropoulos, I. N. *J. Phys. Chem. A* **2004**, *108*, 7291–7300.

(17) Johnson, E. R.; Becke, A. D. *Chem. Phys. Lett.* **2006**, *432*, 600–603.

(18) Subotnik, J. E.; Sodt, A.; Head-Gordon, M. *J. Chem. Phys.* **2006**, *125*, 074116/1–12.

(19) Echenique, P.; Calvo, I.; Alonso, J. L. *J. Comput. Chem.* **2006**, *27*, 1733–1747.

(20) Kaminský, J.; Jensen, F. *J. Chem. Theory Comput.* **2007**, *3*, 1774–1788.

(21) Echenique, P.; Alonso, J. L. *J. Comput. Chem.* **2008**, *29*, 1408–1422.

(22) Gresh, N.; Kafafi, S. A.; Truchon, J.-F.; Salahub, D. R. *J. Comput. Chem.* **2004**, *25*, 823–834.

(23) DiStasio, R. A., Jr.; Jung, Y.; Head-Gordon, M. *J. Chem. Theory Comput.* **2005**, *1*, 862–876.

(24) DiStasio, R. A., Jr.; Steele, R. P.; Rhee, Y. M.; Shao, Y.; Head-Gordon, M. *J. Comput. Chem.* **2007**, *28*, 839–856.

(25) (a) Holroyd, L. F.; van Mourik, T. *Chem. Phys. Lett.* **2007**, *442*, 42–46. (b) Shields, A. E.; van Mourik, T. *J. Phys. Chem. A* **2007**, *111*, 13272–13277.

(26) Polly, R.; Werner, H.-J.; Manby, F. R.; Knowles, P. J. *Mol. Phys.* **2004**, *102*, 2311–2321.

(27) (a) Hampel, C.; Werner, H.-J. *J. Chem. Phys.* **1996**, *104*, 6286–6297. (b) Schütz, M.; Werner, H.-J. *J. Chem. Phys.* **2001**, *114*, 661–681. (c) Schütz, M. *Phys. Chem. Chem. Phys.* **2002**, *4*, 3941–3947. (d) Schütz, M.; Manby, F. R. *Phys. Chem. Chem. Phys.* **2003**, *5*, 3349–3358.

(28) (a) Schütz, M.; Werner, H.-J. *Chem. Phys. Lett.* **2000**, *318*, 370–378. (b) Schütz, M. *J. Chem. Phys.* **2000**, *113*, 9986–10001.

(29) Schütz, M.; Werner, H.-J.; Lindh, R.; Manby, F. R. *J. Chem. Phys.* **2004**, *121*, 737–750.

(30) (a) Hetzer, G.; Pulay, P.; Werner, H.-J. *Chem. Phys. Lett.* **1998**, *290*, 143–149. (b) Schütz, M.; Hetzer, G.; Werner, H.-J. *J. Chem. Phys.* **1999**, *111*, 5691–5705. (c) Hetzer, G.; Schütz, M.; Stoll, H.; Werner, H.-J. *J. Chem. Phys.* **2000**, *113*, 9443–9455. (d) Werner, H.-J.; Manby, F. R.; Knowles, P. J. *J. Chem. Phys.* **2003**, *118*, 8149–8160.

(31) (a) Dunning, T. H., Jr. *J. Chem. Phys.* **1989**, *90*, 1007–1023. (b) Kendall, R. A.; Dunning, T. H., Jr.; Harrison, R. J. *J. Chem. Phys.* **1992**, *96*, 6796–6806.

(32) Werner, H.-J.; Knowles, P. J.; Lindh, R.; Manby, F. R.; Schütz, M.; Celani, P.; Korona, T.; Mitrushenkov, A.; Rauhut, G.; Adler, T. B.; Amos, R. D.; Bernhardsson, A.; Berning, A.; Cooper, D. L.; Deegan, M. J. O.; Dobbyn, A. J.; Eckert, F.; Goll, E.; Hampel, C.; Hetzer, G.; Hrenar, T.; Knizia, G.; Köppl, C.; Liu, Y.; Lloyd, A. W.; Mata, R. A.; May, A. J.; McNicholas, S. J.; Meyer, W.; Mura, M. E.; Nicklass, A.; Palmieri, P.; Pflüger, K.; Pitzer, R.; Reiher, M.; Schumann, U.; Stoll, H.; Stone, A. J.; Tarroni, R.; Thorsteinsson, T.; Wang, M.; Wolf, A. MOLPRO, version 2006. 4; Cardiff School of Chemistry, Cardiff University, Cardiff, UK, 2006.

(33) Frisch, M. J.; Trucks, G. W.; Schlegel, H. B.; Scuseria, G. E.; Robb, M. A.; Cheeseman, J. R.; Zakrzewski, V. G.; Montgomery, J. A., Jr.; Stratmann, R. E.; Burant, J. C.; Dapprich, S.; Millam, J. M.; Daniels, A. D.; Kudin, K. N.; Strain, M. C.; Farkas, O.; Tomasi, J.; Barone, V.; Cossi, M.; Cammi, R.; Mennucci, B.; Pomelli, C.; Adamo, C.; Clifford, S.; Ochterski, J.; Petersson, G. A.; Ayala, P. Y.; Cui, Q.; Morokuma, K.; Malick, D. K.; Rabuck, A. D.; Raghavachari, K.; Foresman, J. B.; Cioslowski, J.; Ortiz, J. V.; Baboul, A. G.; Stefanov, B. B.; Liu, G.; Liashenko, A.; Piskorz, P.; Komaromi, I.; Gomperts, R.; Martin, R. L.; Fox, D. J.; Keith, T.; Al-Laham, M. A.; Peng, C. Y.; Nanayakkara, A.; Gonzalez, C.; Challacombe, M.; Gill, P. M. W.; Johnson, B.; Chen, W.; Wong, M. W.; Andres, J. L.; Gonzalez, C.; Head-Gordon, M.; Replogle, E. S.; Pople, J. A. Gaussian 98, Revision A.7; Gaussian, Inc., Pittsburgh, PA, 1998.

(34) Preusser, A. *ACM Trans. Math. Software* **1989**, *15*, 79–89.

(35) (a) Helgaker, T.; Klopper, W.; Koch, H.; Noga, J. *J. Chem. Phys.* **1997**, *106*, 9639–9646. (b) Halkier, A.; Helgaker, T.; Jørgensen, P.; Klopper, W.; Koch, H.; Olsen, J.; Wilson, A. K. *Chem. Phys. Lett.* **1998**, *286*, 243–252.

(36) Hayano, T. xmo, V 4.0 (MOPAC2002 V1); Fujitsu Ltd., Tokyo, Japan, 2001.

(37) Wang, J.; Wolf, R. M.; Caldwell, J. W.; Kollman, P. A.; Case, D. A. *J. Comput. Chem.* **2004**, *25*, 1157–1174.

(38) (a) Berendsen, H. J. C.; van der Spoel, D.; van Drunen, R. *Comput. Phys. Commun.* **1995**, *91*, 43–56. (b) Lindahl, E.; Hess, B.; van der Spoel, D. *J. Mol. Model.* **2001**, *7*, 306–317. (c) van der Spoel, D.; Lindahl, E.; Hess, B.; Groenhof, G.; Mark, A. E.; Berendsen, H. J. C. *J. Comput. Chem.* **2005**, *26*, 1701–1718.

(39) Sorin, E. J.; Pande, V. S. *Biophys. J.* **2005**, *88*, 2472–2493.

(40) Hornak, V.; Abel, R.; Okur, A.; Strockbine, B.; Roitberg, A.; Simmerling, C. *Proteins: Struct. Funct. Bioinf.* **2006**, *65*, 712–725.

(41) Fujitani, H.; Tanida, Y.; Matsuura, A. Phys. Rev. E 2009, *79*, 021914.

(42) Wang, J.; Cieplak, P.; Kollman, P. A. *J. Comput. Chem.* **2000**, *21*, 1049–1074.

CT8005437